Supporting information

Chemical tailoring of one-dimensional polypyrene nanocapsules on molecular level: towards ideal sulfur hosts for high-performance Li-S batteries

Zhichang Xiao[a,b], Xiaohui Xu[a], Debin Kong[a], Jiaxu Liang[a], Shanke Zhou[a], Xiaoxiong Huang[a], Qi Yang[a], and Linjie Zhi[a]*

a CAS Key Laboratory of Nanosystem and Hierarchical Fabrication, CAS Center for Excellence in Nanoscience, National Center for Nanoscience and Technology, Beijing 100190, P. R. China.

b College of Sciences, Agricultural University of Hebei, Baoding 071001, P. R. China

Contents:

Experimental section

Fig. S1 High resolution TEM image of PPNC.

Fig. S2 (a) Nitrogen adsorption/desorption isotherms at 77.3 K of PPNC and (b) the corresponding pore size distribution calculated using DFT methods.

Fig. S3 Thermogravimetric curve of PPNC in N_2 with a heating rate of 10 K min^{-1}.

Fig. S4 SEM images of (a) PPNC-2 and (b) PPNC-8.

Fig. S5 HRTEM images of PPNC before rinsing.

Fig. S6 TEM image of PCNC.

Fig. S7 (a) SEM image and (b) TEM image of o-PCNC, in which the samples show typical cap-opened character.

Fig. S8 Powder X-ray diffraction (P-XRD) patterns of (a) PPNC and (b) PCNC.

Fig. S9 (a) Nitrogen adsorption/desorption isotherms at 77.3 K of PCNC and (b) the corresponding pore size distribution calculated using DFT methods.

Fig. S10 Cyclic voltammetry (CV) curve of PCNC/S-60 measured between 1.5 and 2.8 V at a sweep rate of 0.05 mV s^{-1} for the first 6 cycles.

Fig. S11 Charge/ discharge profiles of PCNC/S-60 at 2 C.

Fig. S12 Nyquist plots of PCNC/S-60 and o-PCNC/S electrodes.

Fig. S13 Cycling performance of (a) PCNC/S-69.8 and (b) PCNC/S-76.4 at 2 C rate for 200 cycles.

Table S1 The ratios of sp^2 carbon in PPNC and PCNC calculated from the XPS C1s results.

Table S2 Comparison of the reported Li-S battery performance of different porous materials with hollow structure at various current densities.

Experimental Section

1. Sample preparation

Synthesis of PPNC: the synthesis of PPNC-x is carried out by a modified knitting reaction. 0.01 mol (2024 mg) pyrene was dissolved in 10 mL dichloroethane (DCE), which is then added into the solution of $FeCl_3$ (1.6 g, 0.01 mol) and 0.04 mol FDA (3600 μL) in 10 mL DCE. The solution was stirred thoroughly in ice-bath to guarantee a uniform mixture of the monomers. Afterwards, the mixture was consistently stirred at 45 ˚C for 5 h to get original organic networks, and kept at 80 ˚C for 19 h to finish the reaction. When the mixture was cooled down to room temperature, the precipitate was transferred into centrifuge tube and washed with HCl and ethanol for five times till the solution was colourless. Finally, the product was washed with ethanol in a Soxhlet for 24 h, followed by drying in an oven at 60 ℃ overnight.

Synthesis of PPNC-2 and synthesis of PPNC-8 are similar to that of PPNC, except the amount of FDA is 0.02 mol (1800 μL) and 0.08 mol (7200 μL), respectively.

Synthesis of PCNC and o-PCNC: PPNC was pyrolyzed at 800 °C for one hour under argon with the heating rate of 3 ˚C min^{-1} to get PCNC; and o-PCNC was obtained by sonication of PCNC solution (~2.5 mg mL^{-1} in ethanol) for 20 minutes with Ultrasonic Cell Disruptor.

Synthesis of PCNC/S-60, PCNC/S-69.8, PCNC/S-76.4 and o-PCNC/S: The sulfur incorporation procedure was implemented by a sulfur vapor infusion strategy. First, PCNC and sulfur were mixed together with a weight ratio of 4:6, 3:7 and 1:4,

respectively. Second, 1 mL CS_2 was dripped on the sulfur to dissolve it enabling the impregnation. Third, the samples were dried in a fume hood and then put in quartz tubes that were sealed under vacuum. Lastly, the sulfur impregnation was carried out by heating the mixtures in the vacuum-sealed quartz tube under 155 ˚C for 10 hours. For o-PCNC/S, the synthesis is similar except the weight ratio between o-PCNC and sulfur is 4:6.

2. Sample Characterization:

The FTIR spectrum was conducted by Fourier transform infrared spectrometer (FT-IR, Perkin, Spectrum One). The microstructure was analysed by scanning electron microscopy (SEM, Hitachi S4800), Field-emission transmission electron microscopy (FE-TEM, Tecnai G2 F20 U-TWIN), X-ray diffraction (Rigaku D/max-2500B2+/PCX system) and Raman spectra (Renishaw, Renishaw invia plus). Nitrogen sorption isotherms were measured by nitrogen physisorption at 77 K on a Micrometritics ASAP 2020 analyzer. The pore size distribution (PSD) was collected by a density functional theory (DFT) method. Solid-state NMR spectra were determined on a WB 400 MHz Bruker Avance III spectrometer. The ^{13}C CP/MAS NMR spectra were recorded with the contact time of 2 ms (ramp 100) and pulse delay of 3 s. X-ray photoelectron spectroscopy (XPS) measurement was carried out on an ESCALAB250Xi system with a monochromatic Al Kα X-ray source.

3. Electrochemical measurements

PCNC/S, poly (vinylidene fluoride) (PVDF) binder (dispersed in N-methylpyrrolidone) and acetylene black were blended to get a uniform slurry, which was spread onto an aluminum foil and dried in a vacuum oven. After cooling down to room temperature, PCNC/S cathode was obtained. Li-S batteries were assembled in CR2032 coin-type cells. Lithium foil and the Celgard 2400 membrane were put into the cells as anode and seperator, respectively. The electrolyte was prepared by disolving 1 mol L^{-1} lithium bis(trifluoromethanesulfonyl) imide (LiTFSI) and 2 wt% $LiNO_3$ in tetraethylene glycol dimethyl ether (TEGDME). The cycling performance and rate capability were carried out on the Land Battery Measurement System between 1.5-2.8 V. Electrochemical impedance spectroscopy (EIS) and cyclic voltammetry (CV) measurements were conducted on a Bio-logic VMP potentiostat.

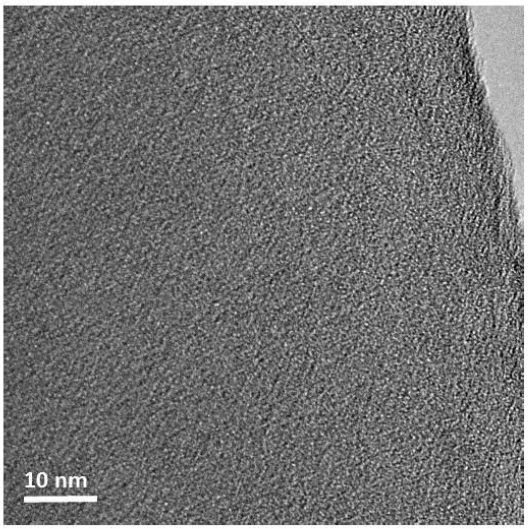

Fig. S1 High resolution TEM image of PPNC.

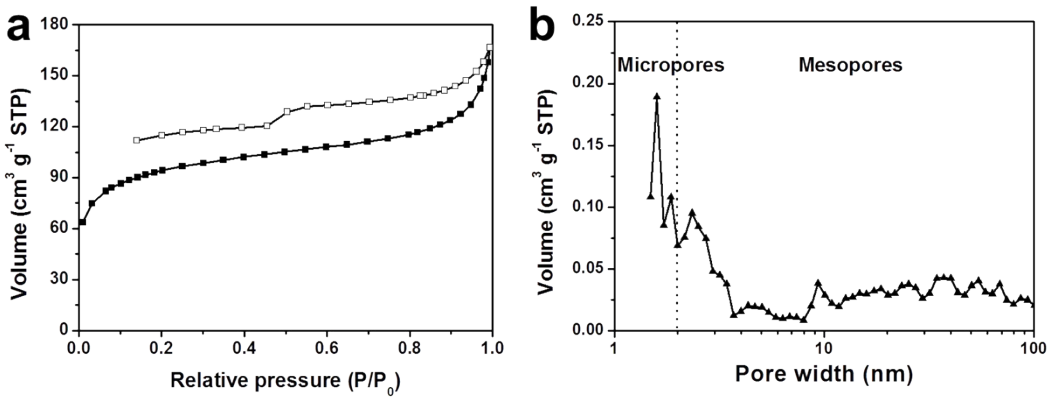

Fig. S2 (a) Nitrogen adsorption/desorption isotherms at 77.3 K of PPNT and (b) the corresponding pore size distribution calculated using DFT methods.

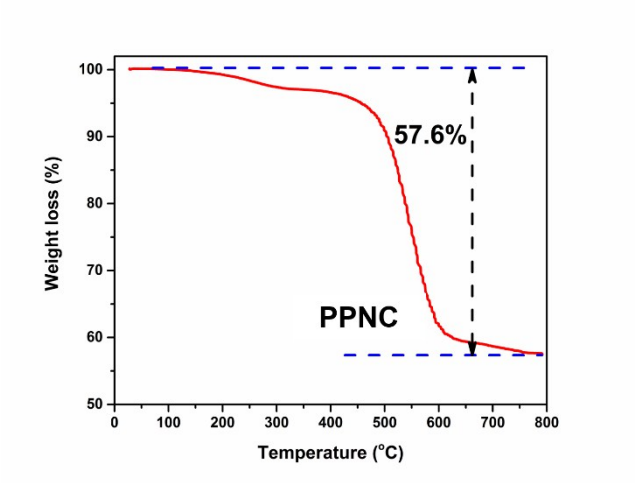

Fig. S3 Thermogravimetric curve of PPNC in N_2 with a heating rate of 10 K min^{-1}.

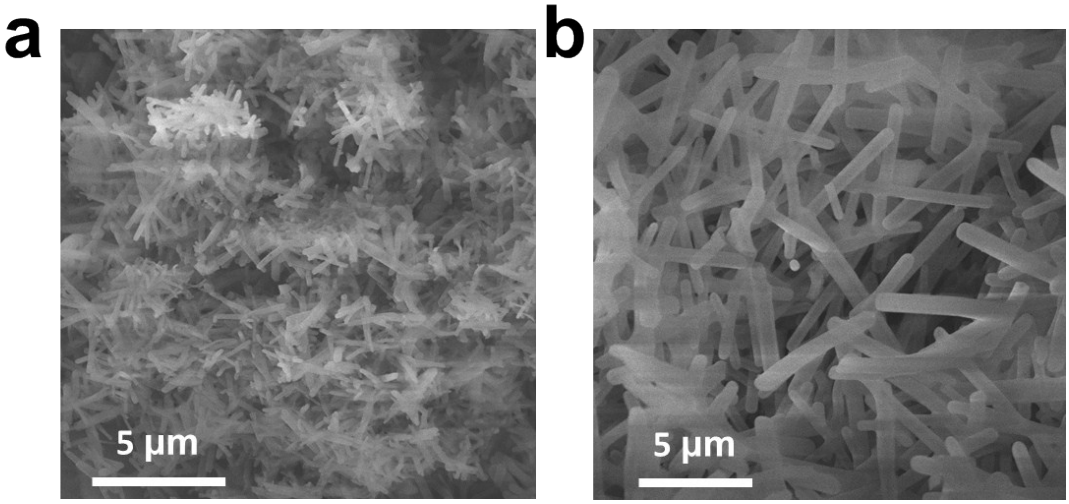

Fig. S4 SEM images of (a) PPNC-2 and (b) PPNC-8.

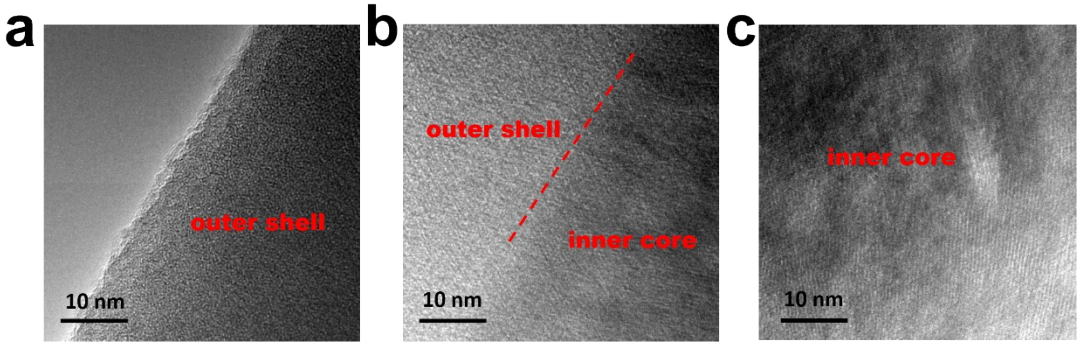

Fig. S5 HRTEM images of PPNC before rinsing.

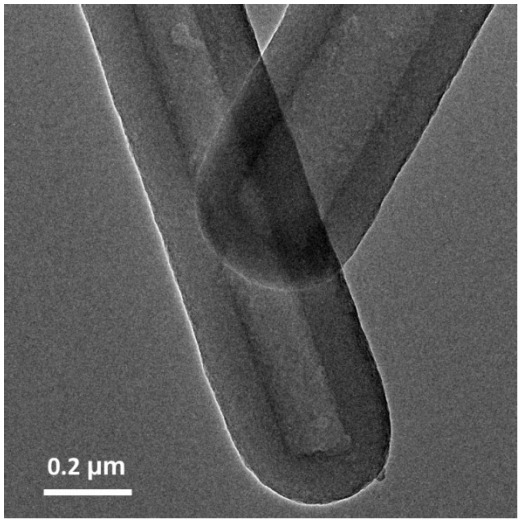

Fig. S6 TEM image of PCNC.

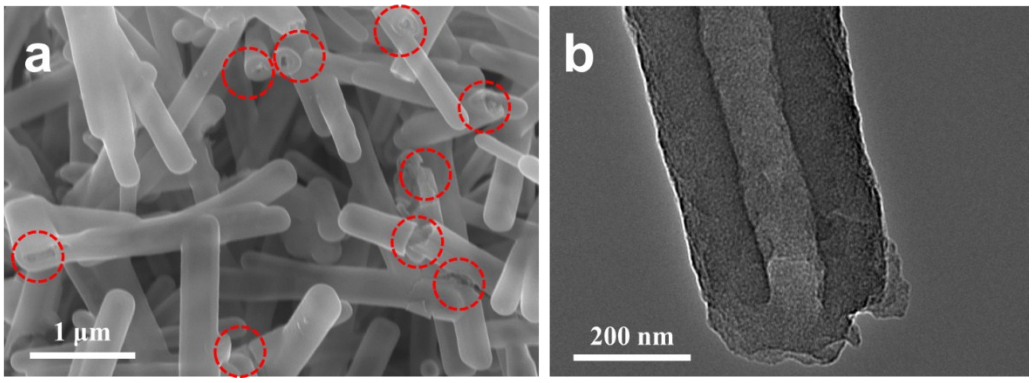

Fig. S7 (a) SEM image and (b) TEM image of o-PCNC, in which the samples show typical cap-opened character.

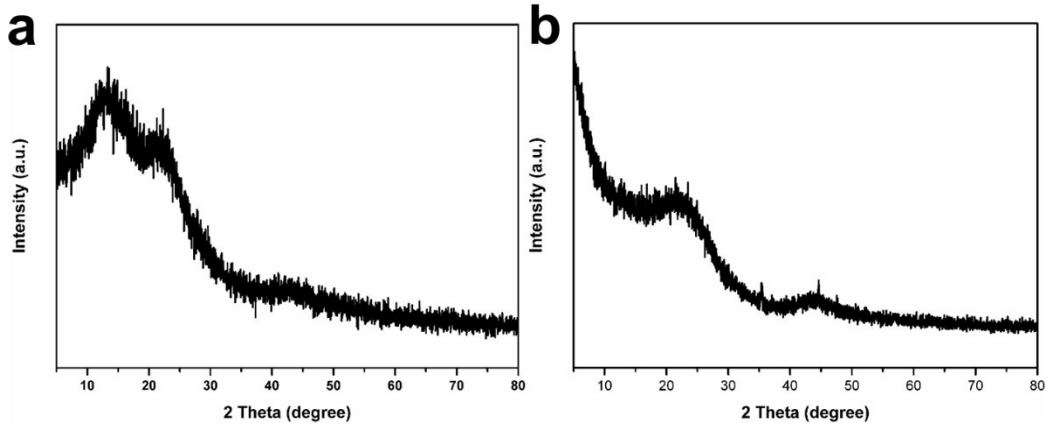

Fig. S8 Powder X-ray diffraction (P-XRD) patterns of (a) PPNC and (b) PCNC.

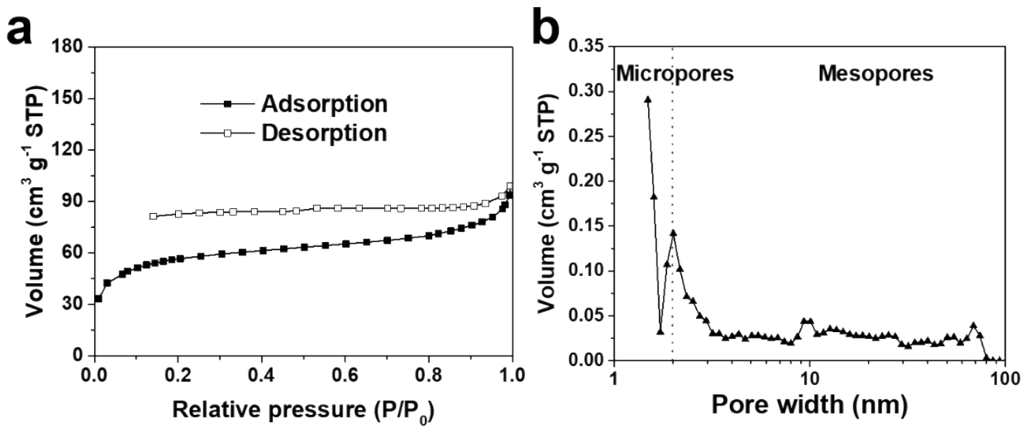

Fig. S9 (a) Nitrogen adsorption/desorption isotherms at 77.3 K of PCNC and (b) the corresponding pore size distribution calculated using DFT methods.

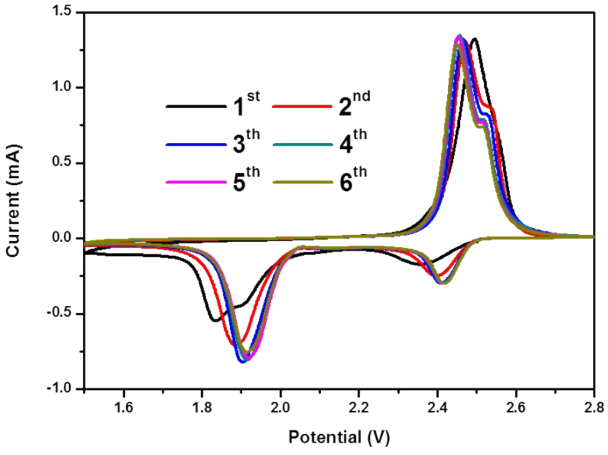

Fig. S10 Cyclic voltammetry (CV) curve of PCNC/S-60 measured between 1.5 and 2.8 V at a sweep rate of 0.05 mV s^{-1} for the first 6 cycles.

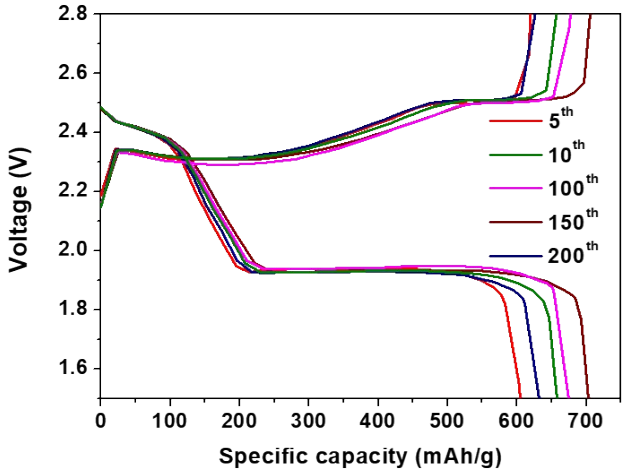

Fig. S11 Charge/discharge profiles of PCNC/S-60 at 2 C.

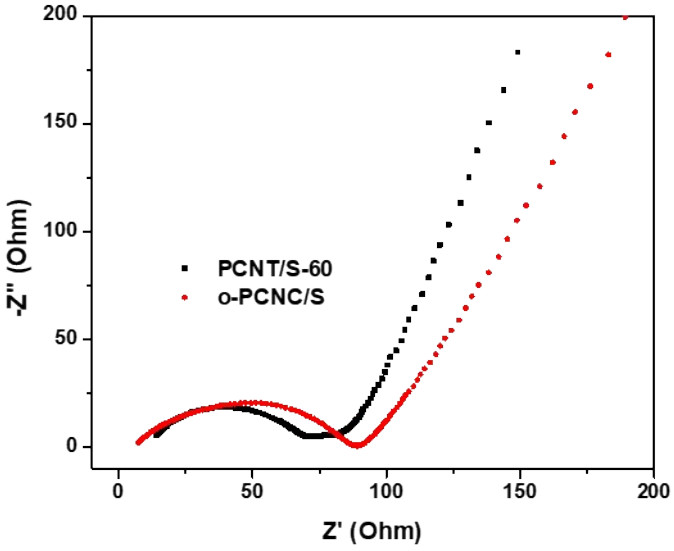

Fig. S12 Nyquist plots of PCNC/S-60 and o-PCNC/S electrodes.

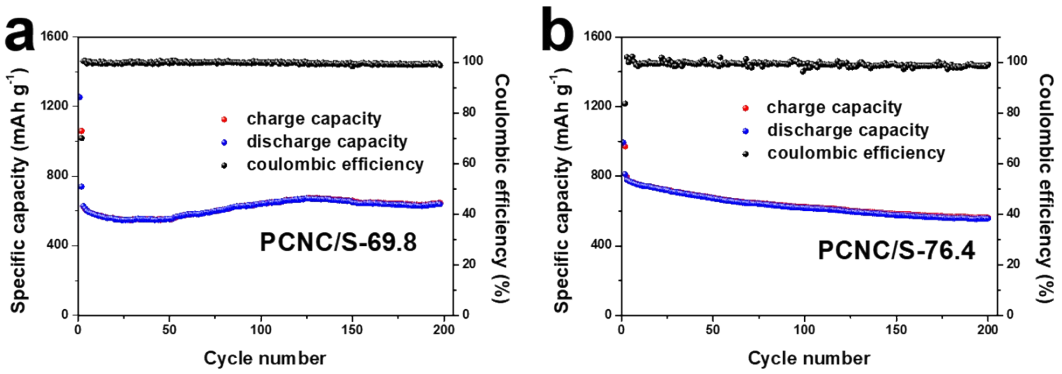

Fig. S13 Cycling performance of (a) PCNC/S-69.8 and (b) PCNC/S-76.4 at 2 C rate for 200 cycles.

Table S1 The ratios of sp^2 carbon in PPNC and PCNC calculated from the XPS C1s results.

Sample	**sp^2 carbon (wt%)**
PPNC	73.66
PCNC	92.34

Table S2 Comparison of the reported Li-S battery performance of different porous materials with hollow structure at various current densities.

Sample	Specific capacity (mAh g^{-1})	Cycle number	Current density/ C-rate	Capacity decay percycle (%)	Reference
PCNC/S	470	800	4 C	0.011	This work
DHCS-S	690	100	0.1 C	0.32	*Angew. Chem. Int. Ed.*, **2012**, *51*, 9592
S/PPy-MnO_2	550	500	1 C	0.07	*Nano Lett.*, **2016**, *16*, 7276
S/YSC@Fe_3O_4	1165	200	0.1 C	0.07	*Adv. Mater.*, **2017**, *29*, 1702707
Li_2S@NCNF	560	200	1 C	0.12	*Adv. Energy Mater.*, **2017**, *7*, 1700018
CF@CNTs/MgO-S	390	800	2 C	0.06	*Adv. Funct. Mater.*, **2017,** *27*, 1702573
HPCR-S	700	300	1 C	0.046	*Adv. Funct. Mater.*, **2016**, *26*, 8952
S/HCN_x	579	500	0.5 C	0.076	*Adv. Mater. Interfaces*, **2017**, 1601195
CNTs/Co_3S_4-NBs	752	500	1 C	0.042	*J. Am. Chem. Soc.*, **2017**, *139*, 12710
S@hCNC	558	300	1 A g^{-1}	0.16	*Nano Energy*, **2015**, *12*, 657
modified hollow carbon nanofiber/sulfur	~662	300	0.5 C	0.067	*Nano Lett.*, **2013**, *13*, 1265
LRC/S@EFG	950	200	0.2 C	0.1	*Nat. Commun.*, **2015**, *6*, 8850
Sulphur-TiO_2 yolk-shell nanostructure	~690	1000	0.5 C	0.033	*Nat. Commun.*, **2013**, *4*, 1331
TiO@C-HS/S	630	500	0.5 C	0.08	*Nat. Commun.*, **2016**, *7*, 13065
Li_2S@graphene	762	200	160 mA g^{-1}	~0.34	*Nat. Energy*, **2017**, *2*, 17090.
Porous Hollow Carbon@Sulfur	974	100	0.5 C	0.09	*Angew. Chem. Int. Ed.*, **2011**, *50*, 5904